

## Preparation of High Flexible Composite Film of Hydroxyapatite and Chitosan

Seong-Hoon Kim<sup>1</sup>, Byoung-Ki Lim<sup>1</sup>, Fangfang Sun<sup>1</sup>, Kwangnak Koh<sup>1</sup>,  
Su-Chak Ryu<sup>1</sup>, Hong-Sung Kim<sup>2</sup>, Jaebeom Lee<sup>1</sup> (✉)

<sup>1</sup> College of Nanoscience and Nanotechnology, Pusan National University, Miryang 607-706, Korea

<sup>2</sup> College of Natural Resources and Life Science, Pusan National University, Miryang 607-706, Korea

E-mail: jaebeom@pusan.ac.kr

Received: 23 April 2008 / Revised version: 17 September 2008 / Accepted: 5 October 2008

Published online: 20 October 2008 – © Springer-Verlag 2008

### Summary

Microscale hydroxyapatite (HAp), a well-known biocompatible substance for the regeneration and reinforcement of damaged bones, was composited with chitosan as a counter-polymer to produce a film with both biocompatibility and flexibility. Homogeneously dispersed solutions of microscale HAp powder and chitosan with various concentrations of HAp and chitosan were prepared in an attempt to optimize the characteristics of the film at room temperature using a molding method. The physiochemical and morphological properties of the prepared film were analyzed by thermal gravimetric analysis, Fourier transform infrared spectroscopy and field emission scanning electron microscopy. The prepared film showed high flexibility with homogeneous distribution of chitosan powders in the whole film. The results suggest that a biocompatible film of microscale HAp can be applied in various fields, such as the surface modification of bone implants, regeneration of damaged bones, osteoporosis to improve biocompatible interface between osteoblast cells and microscale inorganic materials, and to improve the osteoconductivity of bone regeneration

### Introduction

Artificial hydroxyapatite (HAp) has attracted the attention of material scientists and engineers on account its high bio-mimetic properties and similar osteoconduction to innate biomaterials [1-3]. HAp has high biocompatibility, easy-to-shape characteristics and capacity for self-setting. The current use of HAp has expanded to periodontal cements to recover damaged teeth for the preservation and repair of hard tissue defects, and for augmenting edentulous alveolar ridges [4-8]. In particular, HAp pastes were cemented in injured jaw bones and reinforced for subsequent treatments of tooth repair [9-12]. The HAp cement or coating method enhanced the biocompatibility of the interface between the periodontal gum tissue and orthopedic implants. Moreover, the scratched surface of a dental crown was recovered by

immersion in HAp for two or three months [13-16]. However, a practical issue with hydroxyapatite implantation lies in its difficulty in localization due to the tendency of the particles to migrate from implantation sites. In addition, the brittle nature of HAp limits its clinical and dental applications. Hence, the development of biodegradable films with physical flexibility and osteoconductivity would be an obvious advantage [17, 18].

This paper suggests a method for preparing biocompatible and biodegradable films using HAp and chitosan mixtures. Chitosan is a species of polysaccharide with high biocompatibility and biodegradability, and low toxicity with a high cationic potential [19-24]. A mixture solution of HAp and chitosan was optimized by analyzing the zeta potential, as well as the UV-vis and Fourier transform infrared (FT-IR) spectra. The morphology of the prepared film was observed by field emission scanning electron microscopy (FE-SEM).

## Experimental

### *Preparation of HAp films*

HAp powders, which were separated from a 635-mesh ( $\leq 20 \mu\text{m}$ ) sieve, were supplied by HAp Tech Inc. (Pusan, Korea), and used without further purification. The size distribution of the HAp powder was  $3.0 \pm 0.1 \mu\text{m}$  according to a zeta-sizer (ZS-nano, Malvern, United Kingdom). It was reported that the HAp powder showed excellent biocompatibility with hard calcified tissues and was similar to the mineral components of bone [25, 26]. The X-ray diffraction (XRD) revealed peaks at  $31.8^\circ 2\theta$  were, which correspond to the natural HAp according to the Joint Committee on Powder Diffraction Standards (JSPDS) card (# 9-432). ICP-optical emission spectroscopy revealed the weight percentage of CaO and  $\text{P}_2\text{O}_5$  to be 57.0 wt% and 41.4 wt%, respectively. Energy dispersive spectroscopy (EDS) analysis showed a molar Ca/P ratio of 1.67. From quantitative analysis, the composition of the HAp powder utilized for film preparation was similar to the innate HAp in human physiological bone [27]. Chitosan (M.W., 400,000 g/mol, Sigma) was used to fabricate bio-applicable films with HAp.

To prepare the HAp/chitosan composite films, 0.5 g of chitosan powder was dissolved in 50 ml of D.I. water with the pH 1.5~1.8 adjusted with 0.05 M HCl. A low pH was required to prepare a dense chitosan solution in water. The solution was mixed with vigorous magnetic stirring for 1 h at room temperature. The quantity of the HAp powder used was 0.125 g, 0.25 g, 0.5 g, 1 g and 2 g. The HAp powder was mixed into a chitosan dispersed solution with constant stirring. The acidity of the above dispersed solution was adjusted to pH 3.0~3.2 using a 1 M NaOH solution to optimize the homogeneous dispersity of the HAp powders in a chitosan solution. In order to avoid complete ionization of the HAp powders at low pH, the pH was increased slightly after dissolution. The zeta-potentials of the composite solution were measured using a Zeta sizer (ZS-nano, Malvern, United Kingdom) before the drying process in order to determine the surface potential and dispersity of the colloids in the aqueous state. After adjusting the solution pH, 20 ml of the solution was casted in an aluminum Petri dish ( $d$ , 5 cm) in a drying oven for 24 h at room temperature until it naturally peeled off. The dried films were neutralized with a 1.0 M NaOH solution to reduce the concentration of  $\text{H}^+$  ions on the film surface.

### *Characterization of HAp film*

FT-IR reflection absorption spectroscopy (FT-IR RAS 6300, JASCO, Japan) was used to determine the chemical composition of the HAp and chitosan powder in the range of  $4000 \sim 700 \text{ cm}^{-1}$ . The surface morphology was examined by FE-SEM (Hitachi S4700, Japan). The films were dried completely in an automatic desiccator for a 2 - 3 days with a humidity of  $< 10 \%$ . The film surface was coated by Pt sputter prior to imaging. Thermo gravimetric analysis (TGA) (SCINCO model # 1000, Korea) was performed with a 6.00 mg film sample mixture of the prepared HAp-chitosan film from 25 to  $900 \text{ }^\circ\text{C}$  at a rate of  $10 \text{ }^\circ\text{C}/\text{min}$ .

## **Results and Discussions**

### *Zeta potential measurement*

The measured zeta potentials before pH adjustment of the HAp-chitosan solution at pH 1.5 ranged from + 30 to 40 mV. In this pH range, the solution showed a lack of colloidal scattering, which confirmed that the whole HAp micropowders dissolved without any uncontrollable aggregation, opaque light scattering or precipitation. After adjusting the pH to 3.0  $\sim$  3.2 with a 1.0 M NaOH solution, the solution was still transparent without any noticeable precipitation, even though its zeta potential had decreased slightly to + 10  $\sim$  14 mV. The surface potential of the micropowders originated from the partial ionization of the HAp powders and chitosan in solution, which induced a repulsive interaction between the micropowders that can help stabilize the HAp in polymeric solvents.

### *Characterization of film based on different composite ratios*

The HAp-chitosan composite film was prepared using a molding method with different concentration ratios (Table 1). As the water molecules were evaporated, the films began to form from the edge of the aluminum mold. The cross-linking of polymers was observed during the drying step and the recrystallization of HAp powders proceeded in all areas of the dish. Finally, a white colored HAp-chitosan composite film with high flexibility was obtained. At this stage, the film surface was further treated to prevent hydrolysis by neutralization with  $\text{OH}^-$  ions to remove  $\text{H}^+$  ions from the film surface. The drying time, temperature, and concentration of the solution were the essential factors examined. The optimal conditions were investigated to ensure uniformity of the composites (without phase separation), surface homogeneity, and appropriate flexibility. The weight % of HAp and chitosan was measured from the tendency of pyrolysis using TGA analysis. The water content was approximated from a representative TGA experiment of the films prepared under the same conditions as the drying process. According to the table, the appropriate water content was important for sustaining the flexible polymer film. The threshold concentration ratio of HAp and chitosan used was 1:4, 1:1 and 2:1 to avoid phase separation, which would induce film brittleness. The chitosan in the polymeric matrix supported the flexible characteristics while micro-size HAp particles were trapped uniformly in the polymeric scaffold matrix. After a NaOH treatment, the films were marginally sustained without redissolution or degradation by hydrolysis, which might

**Table 1.** Physical and morphological properties of the prepared HAp-chitosan composite films at various compositions and drying conditions

Sample	Concentration			Water content (w% approx.)	Homogeneity	Flexibility
	HAp w%	chitosan w%	Ratio			
HC 1	20	80	1 : 4	0	Excellent	Poor
HC 2	33	66	1 : 2	0	Excellent	Poor
HC 3	50	50	1 : 1	0	Excellent	Poor
HC 4	66	33	2 : 1	0	Excellent	Poor
HC 5	80	20	4 : 1	0	Excellent	Poor
HC 6	18	72	1 : 4	10	Excellent	Excellent
HC 7	30	60	1 : 2	10	Excellent	Excellent
HC 8	45	45	1 : 1	10	Excellent	Excellent
HC 9	60	30	2 : 1	10	Excellent	Excellent
HC 10	72	18	4 : 1	10	Excellent	Poor
HC 11	16	64	1 : 4	20	Excellent	Excellent
HC 12	27	53	1 : 2	20	Intermediate	Excellent
HC 13	40	40	1 : 1	20	Intermediate	Excellent
HC 14	53	27	2 : 1	20	Intermediate	Intermediate
HC 15	64	16	4 : 1	20	Poor	Poor

allow the use of HAp powder delivery patches or carriers for the osteoconduction of bone regeneration.

#### *Morphology of HAp-chitosan composite films*

Figure 1 shows an image of the fabricated HAp-chitosan composite film. Because of the well-dispersed HAp powders in the polymer matrix, the apparent film appeared white and flexible with a transmittance < 20 % in the visible range. The morphological observation of the FE-SEM images ensured monodispersity of the films. Monodispersity can increase the level of homogeneity and uniformity of the film by preventing phase separation resulting in unwanted microcracks. The FE-SEM images showed that an abundance of spherical particles, which increased with increasing relative HAp concentration. When the HAp and chitosan ratio was increased to 2:1, the film showed excellent homogeneous dispersity of the HAp powders over the entire film area. It is possible that the threshold weight % of HAp in the polymer films was approximately 50~60 % when the film contains 10 ~ 15% moisture. Although HAp itself has little flexibility making it difficult to fabricate a film, the formation of composites using chitosan polymers with suitable moisture can impart excellent flexibility.

#### *FT-IR Spectroscopy*

Figure 2 shows the FT-IR RAS spectra of the HAp and chitosan powders from 4000 ~ 700 cm<sup>-1</sup>. The spectrum of the HAp powder showed a remarkable strong band near

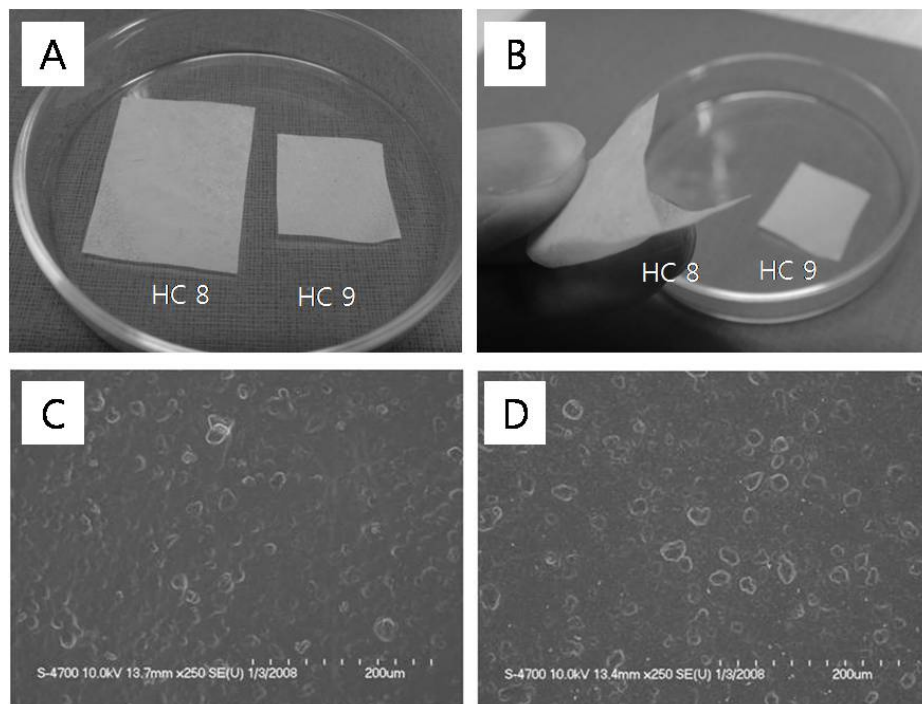


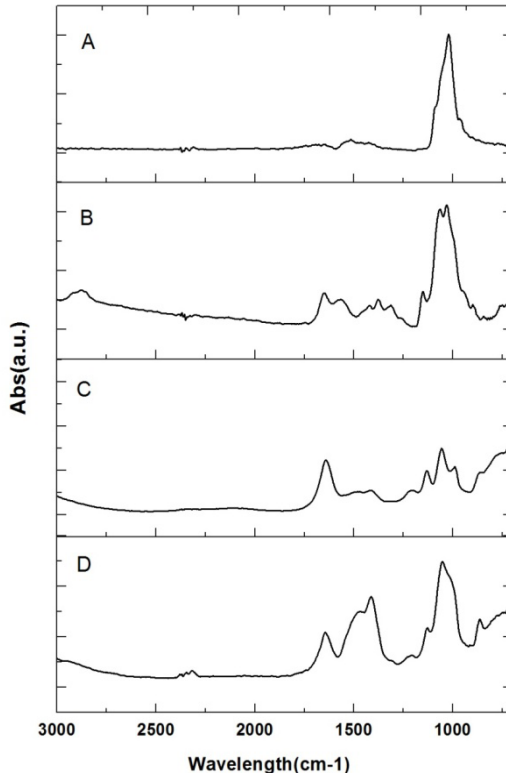
**Figure 1.** (A) The HAp-chitosan films prepared at different concentration ratios. (B) Demonstration of flexibility of HC 8. FE-SEM image of (C) HC 8, and (D) HC 9

$1020\text{ cm}^{-1}$  corresponding the symmetric and asymmetric stretching vibrational mode of  $\text{PO}_4^{3-}$  (Figure 2A). The low intensity of the imperceptible bands at  $1650\text{ cm}^{-1}$  was assigned to the O-H in-plane bending mode [28]. The broadness of the bands may result from restriction of the molecular vibration of ionized  $\text{PO}_4^{3-}$  on the micropowders as well as the ionic interaction with cationic ions. The chitosan polymer (Figure 2B) presented absorption bands observed at  $2875$ ,  $1650$  and  $1565\text{ cm}^{-1}$  were assigned to methyl ( $-\text{CH}_2$ ), amide ( $\text{C}=\text{O}$ ) and amino ( $-\text{NH}_2$ ), respectively [29, 30]. the band intensity near  $1000\text{ cm}^{-1}$  increased with increasing relative HAp concentration in the prepared film, and was attributed to overlapping of the strong bands at  $1020\text{ cm}^{-1}$  induced by the vibrational modes of  $\text{PO}_4^{3-}$  (Figure 2C and D).

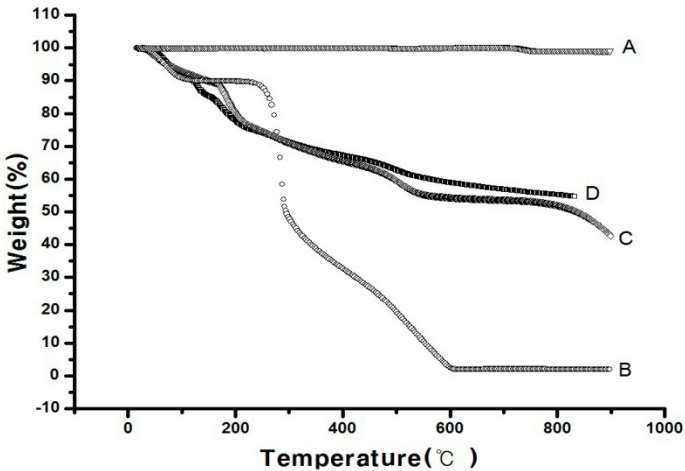
#### *Thermal gravimetric analysis*

Figure 3 shows the TGA data of HAp and chitosan and their composite film. The TGA data of the HAp powder showed high thermal stability with  $< 1\%$  weight loss while the chitosan powder showed three different weight losses at  $\sim 100^\circ\text{C}$ , near  $300^\circ\text{C}$ , and  $300 \sim 600^\circ\text{C}$ . In the first stage near  $100^\circ\text{C}$ , a gradual  $10\%$  weight loss was observed indicating the evaporation of adsorbed water and lattice water [30]. The second and the third stage showed a sudden  $40\%$  weight loss and a gradual weight loss, respectively. The observation of a gradual decrease at near  $300^\circ\text{C}$  and  $500^\circ\text{C}$ , indicated the decomposition of chitosan [31, 32]. The TGA graph of the films showed a relatively lower rate of weight reduction than that of the raw materials. In addition, the decomposition rate, which depends on the thermo stability of the films, decreased

with increasing HAp concentration. This suggests that a dense HAp concentration in the film increases the thermo stability of the films.



**Figure 2.** FT-IR spectra of (A) HAp powder, (B) chitosan polymer, and different composite of HAp/chitosan films of (C) HC 8, and (D) HC 9



**Figure 3.** TGA graph of (A) HAp powder, (B) chitosan powder, (C) HC 8, and (D) HC 9

## Conclusion

A high flexible HAp-chitosan composite film was prepared using homogeneously dispersed solutions of microscale HAp powder and chitosan at various concentrations. The films can contain up to 70 % HAp without microcracks, phase separation and brittleness. FE-SEM showed that the HAp powders were well dispersed in the film without clustering or aggregation. FT-IR revealed the characterized bands of the chitosan polymers. These observations were explained by the chitosan polymers being a strong scaffolding matrix that retains the physio-mechanical properties of the film and captures the microscale HAp powders in the spaces in the matrix. It is anticipated that these films will be potentially useful for the direct or indirect delivery of HAp materials in localized areas of osteoporosis via a patch on skin or bone.

*Acknowledgements.* This work was supported by PNU-IGB joint research center grant and PNU Research Grant, 2007.

## References

1. Y Ohbayashi, M Miyake, S Nagahata (2000) *Biomaterials* 21:509
2. S Itoha, M Kikuchib, Y Koyamac, K Takakudac, K Shinomiyaa, J Tanaka (2002) *Biomaterials* 23:3919
3. YG Kim, DS Seob, JK Lee (2008) *J Phys Chem Solids* 69:1556
4. James B. Thompson, Johannes H. Kindt, Barney Drake, Helen G. Hansma, Daniel E. Morse, Paul K. Hansma (2001) *Nature* 414:773
5. T Kobayashi, S Nakamura, K Yamashita (2001) *J Biomed Mater Res* 57:477
6. C. Guo, H. Liu and I. Katayama (2002) *J Dent Res.* 81:254
7. K. Onumaa, K. Yamagishi and A. Oyane (2005) *J Cryst Growth* 282:199
8. Uchida A, Araki N, Shinto Y, Yoshikawa H, Ono K, Kurisaki E (1990) *J Bone Joint Surg* 72-B:298
9. JA Jansen, JE De Ruijter, HG Schaeken, JPCM Van Der Waerden, JA Planell, FCM Driessens (1995) *J Mater Sci : Mater Med* 11:653
10. Oktar FN, Kesenci K, Pişkin E (1999) *Artif Cells Blood Substit Immobil Biotechnol* 27:367
11. GL De Lange, C De Putter, FLJA De Wijs (2004) *J Biomed Mater Res* 24:829
12. P Ducheyne, K De Groot (2004) *J Biomed Mater Res* 15:441
13. SC. Ryu, BK. Lim, SH. Kim, H. Chen, K. Koh, YH. Hwang, HS. Kim, J. Lee (2008) *Dent Mater*, submitted
14. D Lamy, AC Pierre, RB Heimann (1996) *J Mater Res* 11:680
15. KA Gross, CC Berndt (1994) *J Mater Sci : Mater Med* 5:1573
16. JE Dalton, SD Cook, KA Thomas and JF Kay (1995) *J Bone Joint Surg Am* 77:97
17. I Yamaguchi, K Tokuchi, H Fukuzaki, Y Koyama, K (2001) *J Biomed Mater Res* 55:20
18. Cooke FW (1992) *Clin Orthop Rel Res* 276:135
19. Prudden JF, Migel P, Hanson P, Friedrich L, Balassa L (1970) *Am J Surg* 119:560
20. Lahiji A, Sohrobi A, Hungerford DS, Frondoza CG. (2000) *J Biomed Mater Res* 51: 586
21. Mori T, Okumura M, Matsuura M, Ueno K, Tokura S, Okamoto Y, Minami S, Fujinaga T (1997) *Biomaterials* 18:947
22. Mori T, Irie Y, Nishimura SI, Tokura S, Matsuura M, Okumura M, Kadosawa T, Fujinaga T. (1998) *J Biomed Mater Res* 43:469
23. Sechrist VF, Miao YJ, Niyibizi C, Westerhausen-Larson A, Matthew HW, Evans CH, Fu FH, Suh JK (2000) *J Biomed Mater Res* 49: 534
24. PJ VandeVord, HWT Matthew, SP DeSilva, L Mayton, B (2002) *J Biomed Mater Res* 59:585

25. H. Aoki (1991) *Science and Medical Applications of Hydroxyapatite*. Takayama Press System Center Co. Inc., Tokyo
26. SC. Ryu, BK. Lim, HS. Kim, YM. Park (2007) *Kor J Mater Res* 17:544
27. S. Joscheka, b, B. Niesa, R. Krotzc, A. Göpferich. (2000) *Biomaterials* 21:1645
28. A. Stoch, A. Brozek, S. Błazewicz, W. Jastrzebski, J. Stoch, A. Adamczyk, I. Roj, J (2003) *J Mol Struct* 651–53:389
29. MC Chang, J Tanaka (2002) *Biomaterials* 23:4811
30. M. Ashok, N. Meenakshi Sundaram, S. Narayana Kalkura. (2003) *Materials Letters* 57:2066
31. T. Toyama, T. Dokushima, T. Yasue, Y. Arai (1998) *Inorg Mater* 5:479
32. Qu X, Wirse'n A, Albertsson AC (2000) *Polymer* 41:4841